



HAL
open science

Modeling and control of a hybrid PV-T collector using machine learning

Zain Ul Abdin, Ahmed Rachid

► **To cite this version:**

Zain Ul Abdin, Ahmed Rachid. Modeling and control of a hybrid PV-T collector using machine learning. 31st Mediterranean Conference on Control and Automation, Jun 2023, Limassol, Cyprus. hal-04143400

HAL Id: hal-04143400

<https://hal.science/hal-04143400>

Submitted on 27 Jun 2023

HAL is a multi-disciplinary open access archive for the deposit and dissemination of scientific research documents, whether they are published or not. The documents may come from teaching and research institutions in France or abroad, or from public or private research centers.

L'archive ouverte pluridisciplinaire **HAL**, est destinée au dépôt et à la diffusion de documents scientifiques de niveau recherche, publiés ou non, émanant des établissements d'enseignement et de recherche français ou étrangers, des laboratoires publics ou privés.

Modeling and control of a hybrid PV-T collector using machine learning

Zain Ul Abdin and Ahmed Rachid

Abstract—Photovoltaic-thermal (PV-T) systems are expected to fulfil an increasingly vital role in future energy production. The current research endeavors to showcase machine learning modeling and control of a water-based PV-T collector. In this work, the PV-T collector is modeled using a decision tree algorithm and artificial neural network (ANN). The predicted outputs are compared with the actual outputs to validate the models. The ANN-based model performed better and proved its efficacy in training and testing. Further, various control strategies are implemented and their performance is compared. All the techniques presented are illustrated through simulation results.

Index Terms—PV-T collector, modeling, decision tree algorithm, artificial neural network, control

I. INTRODUCTION

Artificial intelligence (AI) and solar energy are emerging technologies and are expected to grow rapidly. AI is a machine's ability to perform tasks that require intelligence e.g., digital assistants, vehicle recognition and identification, etc. Machine learning is a sub-field of AI that allows the machine to learn and improve from past experiences and data to identify patterns and make predictions. On the other hand, photovoltaic-thermal (PV-T) collector is popular renewable energy technology for homeowners [1]. A PV-T system combines a photovoltaic (PV) module and solar thermal (ST) module into one integrated unit to provide heat and low-carbon electricity simultaneously. The working fluid mostly flows below the PV module and it is not only used for heating purposes but also enhances the PV efficiency by extracting the heat from the PV module. Various studies have been conducted and a variety of different design configurations of PV-T collectors are addressed in the literature. The performance of a PV-T collector is evaluated both numerically and experimentally [2], [3], [4], [5]. A water-based PV-T collector with numerous flow designs is a common domestically used panel and produces more energy than individual conventional PV and ST panels installed over the same area [6]. These systems have various potential applications such as drying, heating, cooling, etc [7], [8], [9]. These collectors are associated with a number of drawbacks, including technically more complex, having corrosion issues, low heat transfer compared to other liquids and a large storage capacity is required.

Zamen *et al.* [10] implemented three different intelligent algorithms that are multilayer perceptron artificial neural network (ANN), adaptive neuro-fuzzy inference system, and least squares support vector machine by constructing a

relationship between thermal efficiency of solar collector and inlet temperature, flow rate, and solar radiation. The findings revealed that the neural network model gave the best performance compared to the other two models. A new model for predicting the performance of the PV-T system incorporated with electrolytic hydrogen production was presented by Elaziz *et al.* [11]. The optimized model was based on a modified version of the random vector functional link, in which Mayfly-based optimization is applied as an optimization technique to determine the best parameters. The ANN-based model was presented by Ravaee *et al.* [12] to evaluate the thermal and electrical performance of a PV-T system. The results confirmed that the ANN could be used as a powerful tool for PV-T collectors modeling. A comparison between multiple learning algorithms methods to forecast the performance evaluation criteria of building integrated PV-T was presented in [13] and it was observed that the random forest model is superior to other proposed models. The efficiency of a semi-transparent air-based photovoltaic thermal double pass collector was compared with a single pass air-based collector using an artificial neural network approach for the New Delhi weather station [14]. The model was based on a feed-forward back propagation algorithm with two hidden layers and a fair agreement was observed between the analytical and ANN models. Neural networks have been applied to a number of industrial applications, such as the improvement of thermal comfort indices accurately [15]. A reference-model-based neural network controller with integral-proportional-derivative compensation has been proposed by Xu *et al.* [16] for temperature control systems.

In this paper, two different approaches are used to model water-based PV-T collector and numerous control schemes are provided based on neural network. The two developed artificial intelligent models are presented in section 2. In section 3, control strategies are presented leading to a precise tracking of the system's desired reference signal. Simulation results are given in section 4 to highlight the usefulness of the proposed design. The paper ends with conclusive remarks and perspectives.

II. PHYSICAL MODELING

A solar hybrid water-based PV-T collector that is composed of several layers; a protective transparent glass cover, a mono-crystalline PV cell layer, a protective tedlar layer below the cells, an absorber, water tubes, fluid that flows within the tubes (mostly water) and thermal insulation to reduce heat losses as illustrated in Fig. 1.

Both authors are with Laboratoire des Technologies Innovantes, Université de Picardie Jules Verne, Amiens, 80000, France. zain.ul@u-picardie.fr and rachid@u-picardie.fr

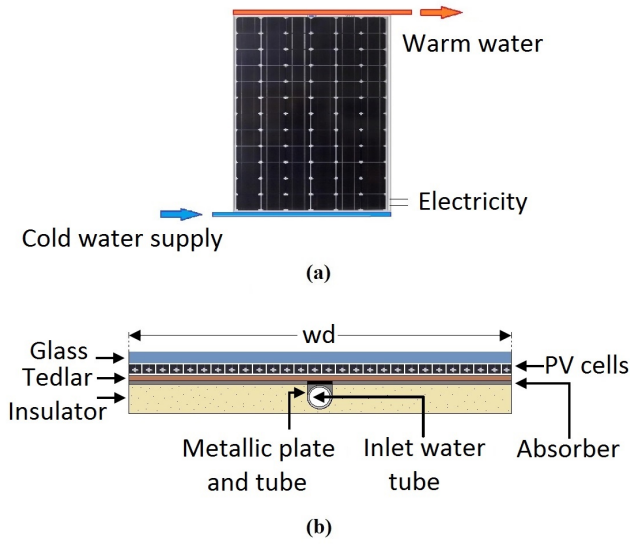


Fig. 1: Water-based photovoltaic-thermal collector [5].

A. Thermal model

A dynamic thermal model of a water-based PV-T collector considering radiative, convective and conductive thermal exchanges between the layers is given in [5]. The fundamental equation for each of the layer is determined using a bond graph approach. The mean temperature with inlet temperature T_{wi} and output temperature of the water channel T_{wo} and can be expressed as;

$$T_w = \frac{(T_{wi} + T_{wo})}{2} \quad (1)$$

Applying useful energy gain, the thermal performance η_{th} of PV-T collector is;

$$\eta_{th} = \frac{\dot{m}_w C_w (T_{wo} - T_{wi})}{A_{mod} I_{sun}} \quad (2)$$

The electric power E_p produced by PV module [4] can be written as;

$$E_p = I_{sun} A_{mod} \eta_r \left[1 - \beta_p (T_c - T_{c,r}) + \delta \ln \left(\frac{I_{sun}}{I_{sun,r}} \right) \right] \quad (3)$$

and electrical efficiency η_{pv} can be then expressed as;

$$\eta_{pv} = \frac{E_p}{A_{mod} I_{sun}} \quad (4)$$

The thermal model can be expressed using a general nonlinear state space form

$$\begin{cases} \dot{x} = f(x, u, p) \\ y = g(x, u) \end{cases}, \quad (5)$$

where the state x contains the temperatures of each layer as state variables. For instance, in this case of water-based PV-T, it is

$$x = [T_g \ T_c \ T_t \ T_r \ T_m \ T_w \ T_i]^T,$$

the control input u is the mass flow rate \dot{m}_w and p are the perturbations,

$$p = [T_{am} \ I_{sun} \ T_{wi}]^T$$

and the output y is the outlet temperature T_{wo} .

The state-space description is useful for the simulation of the system's dynamic behavior and will allow us to generate the input-output data which are necessary for the learning process. Here, four inputs (i.e, solar radiation I_{sun} , ambient temperature T_{am} , wind speed V_w and mass flow \dot{m}_w) and two outputs (i.e., outlet water temperature T_{wo} and electrical efficiency η_{pv}) are considered. Simulations are performed for the water-based model and the values of the two outputs are obtained by considering the inputs data.

B. Decision tree algorithm

A decision tree makes use of input-output data sets to train models and the algorithm determines the contribution value of input parameters [17]. A regression model is built in the form of a tree structure and the goal is to develop a model that predicts the target variable based on several input variables. The data is split using a binary tree and starts at the root node until left with leaf nodes or terminal nodes. A regression model is used and a multi-output decision tree algorithm is implemented in this study. The model can be developed using the following steps:

- import data set;
- separate the target variable;
- split data into a train set and a test set (see Fig. 2);
- scaling is done using a min-max function;
- model creation and implementation (decision tree multi-output regressor is used);
- mean squared error (MSE) and accuracy are calculated;
- lastly, validation is done using the test data.



Fig. 2: Schematic representation.

The data can be expressed in the form:

$$(I, Y) = (I_1, I_2, I_3, I_4, Y_1, Y_2) \quad (6)$$

Y is the target and dependent variable whereas I consists of features that are used for the task. Mean squared error is the average squared difference between actual value and the estimated value and is written as:

$$\text{MSE} = \frac{1}{n} \sum_{i=1}^n (Y_i - \hat{Y}_i)^2, \quad (7)$$

where n is the sample size, Y_i is the actual value of i^{th} case and \hat{Y}_i represents the predicted value of i^{th} case. Similarly, root-mean square error (RMSE) is calculated using [18]:

$$\text{RMSE} = \sqrt{\text{MSE}}. \quad (8)$$

C. Artificial neural network

ANNs have high learning ability and the capability of identifying complex nonlinear systems. Hence, the ANN modeling technique is used, as a powerful tool, to predict and determine the thermal output and photovoltaic efficiency of the collector. In a multilayer neural network, one or more hidden layers are utilized in order to obtain accurate results. The network consists of an input, output and at least one hidden layer sandwiched between the input and output layers as illustrated in Fig. 3 where the data processing is done. Here, there are four input nodes and the output of the linear combiner is the sum of the product of all the inputs with their respective weights and is written as:

$$y = \sum_{i=1}^n W_i I_i, \quad (9)$$

whereas the output signal becomes

$$Y = f(y - T_h) \quad (10)$$

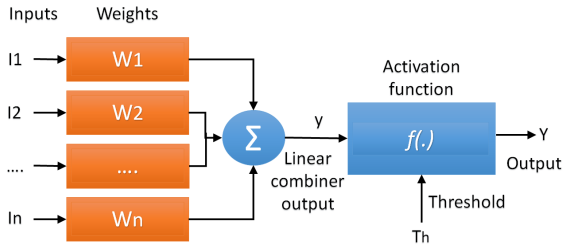


Fig. 3: Typical structure of the neural network.

The output of the neural network is compared with the target output and the difference between the two is computed which is the error. The process is continued until the error converges to zero or the difference is within the target threshold and when it is achieved the neural network is trained. For training, only input-output data is required and based on this data, the neural network understands and learns the relation between input and output.

III. NEURAL NETWORK BASED CONTROL

A neural network is an effective tool for highly nonlinear systems and from the control point of view, it can be taken into consideration as a nonlinear dynamic block. Its performance is generally better than conventional control methods. In this section, numerous controllers based on neural network approach are discussed with the aim to control the temperature of the PV-T water output. The presented techniques are practical and simple to construct and implement the controller.

A. Basic neural network controller

In this part, an artificial neural network-based control system is presented and the approach is to train the controller by collecting data through simulations. Since the aim is to track the desired water temperature and control the

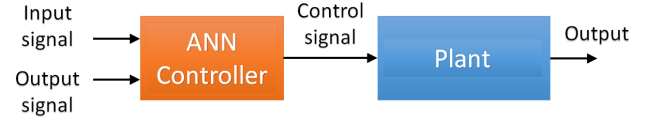


Fig. 4: Scheme for basic neural network controller implementation.

mass flow, so for training, the outputs are mass flow and PV efficiency whereas solar radiation, ambient temperature, wind speed and outlet temperature are chosen as inputs. The ANN goes into the training process for its learning and understanding the relationship between the inputs and outputs. Once the network is trained, the reference value for the output temperature is set and the obtained mass flow can be directly injected to the nonlinear model. Basically, the controller is trained as an inverse model of the system and connected to it as shown in Fig. 4.

B. Neural network predictive control

In this part, a neural network model predictive controller for the system described in section 2 is presented. It is basically a type of model-based predictive control, where the model for predictions is a neural network. It is based on solving an optimization problem for the control actions [19]. The optimizer computes future control actions that minimize the difference between a model of the system and desired performance. Two steps are involved; system identification of the plant model, which is a multilayer network where the network is trained and control design where the control input is calculated by the controller that will optimize the system's performance over a specified time. The predictions are used within an optimization algorithm to determine the control signal. For the reason that optimization algorithm is used, the controller requires a substantial amount of on-line computation. The control evaluation consists of the minimization problem of the following performance criterion:

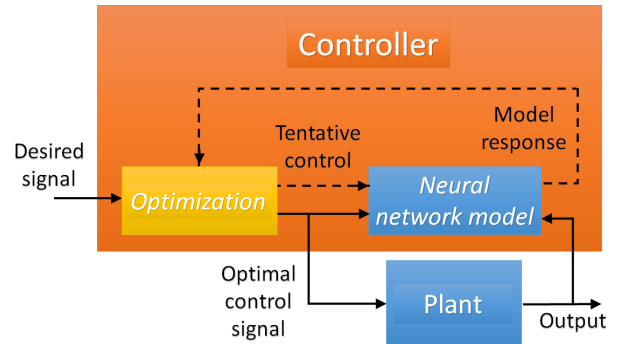


Fig. 5: Structure of model predictive control process.

$$J = \sum_{i=n_1}^{n_2} (y_d(t+i) - y_m(t+i))^2 + \zeta \sum_{i=1}^{n_u} (\bar{u}(t+i-1) - \bar{u}(t+i-2))^2, \quad (11)$$

where \bar{u} is the tentative control signal determined by the optimization block and minimizes the performance index J , n is the prediction horizon for output (e.g. n_2 : cost horizon & n_u : control horizon), y_d is the desired signal and y_m is the neural network model signal. The optimal control signal u is injected into the plant and ζ determines the contribution on the performance index. The block scheme of the model predictive control process is illustrated in Fig. 5.

C. NARMA-L2 control

In this part, nonlinear moving average autoregressive-linearization level 2 (NARMA-L2) control also referred to as feedback linearization control is presented for the described system. It transforms nonlinear system dynamics into linear dynamics by cancelling the non-linearities. Similar to neural network predictive control, the first step is system identification. NARMA is a standard model and mimics the behavior of a discrete-time non-linear system. The control input $u(k)$ must be determined based on output $y(k)$ at the same time and the model of the given form is used [20].

$$y(k+a) = f[Y, U] + g[Y, U]u(k+1), \quad (12)$$

where $a \geq 2$ and the two sub-functions, f and g are the two functions of previous inputs and outputs. This model representation is used in the form of past, current and future system parameters. The relation between the control input and the output is linear and the control input is determined easily. Using the NARMA-L2 model, the controller can be expressed as:

$$u(k+1) = \frac{y_d(k+a) - f[Y, U]}{g[Y, U]}, \quad (13)$$

which is realizable for $a \geq 2$.

$$Y = [y(k), y(k-1), \dots, y(k-n+1)] \quad (14)$$

and

$$U = [u(k), u(k-1), \dots, u(k-n+1)], \quad (15)$$

where $y_d(k+a)$ is the reference signal for output at a time steps ahead. If the plant is a minimum phase system and the relative degree is well defined, the closed loop system is stable. The structure of the controller is given in Fig. 6 where TDL (Tapped Delay Line) supplies the signal at each specified time delay.

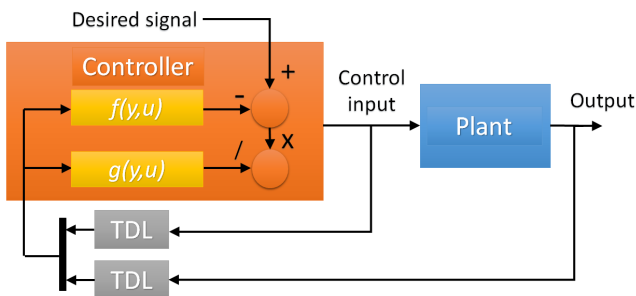


Fig. 6: Structure of NARMA-L2 controller.

IV. RESULTS AND DISCUSSION

Simulink and Matlab program are used to model and test control algorithms for the system. The findings of this work are divided into two sections. In the first section, comparative results of the decision tree algorithm and neural network are presented while in the second section neural network-based control results are discussed. The upper and lower bounds of the inputs are presented in Table I and the aim is to develop a model which must work within these limits.

TABLE I: Lower and upper bounds of input variables.

Input variable	lower bound	upper bound
I_{sun} (Wm^{-2})	100	700
T_{am} ($^{\circ}C$)	21	31
V_w (ms^{-1})	1	5
\dot{m}_w (kgs^{-1})	0.005	0.05

In the decision tree algorithm, 70% of the data is used for learning whereas 30% of the dataset is employed as test data and is later used for validation purpose. An accuracy score of 75% is achieved with a mean squared error of 1.14×10^{-2} and the root mean square error calculated is 0.107. The obtained results in Fig. 7 are satisfactory and indicate that there is under-fitting and the actual results are not accurately predicted. Therefore, in order to predict the outputs accurately, ANN is a good solution to move forward.

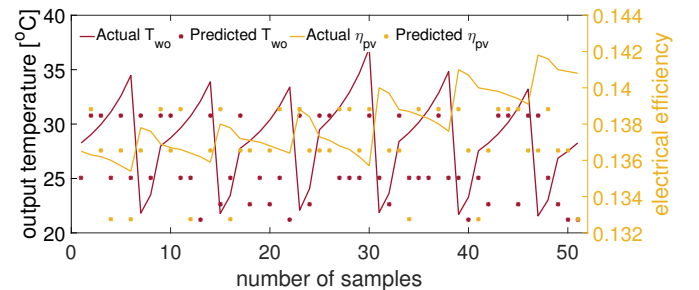


Fig. 7: Comparison of actual and predicted outputs using decision tree algorithm.

In the developed neural network, there are three layers with the visible input layer having four neurons, two neurons for the output layer and sixteen neurons for the hidden layer that is sandwiched between the input and output layers. For the training purpose, Levenberg-Marquardt Backpropagation algorithm is used because of its fast and accurate results. The threshold limit or the convergence limit, in this case, is 1×10^{-7} . The performance is checked using mean squared error and the best performance is successfully reached.

The results found in Fig. 8 show that the actual outputs are accurately predicted using a neural network. There are minor differences in the PV efficiency output but the output water temperature is accurately predicted for all the samples.

The initial results showed that the outputs are accurately and efficiently predicted. Random input values as shown in

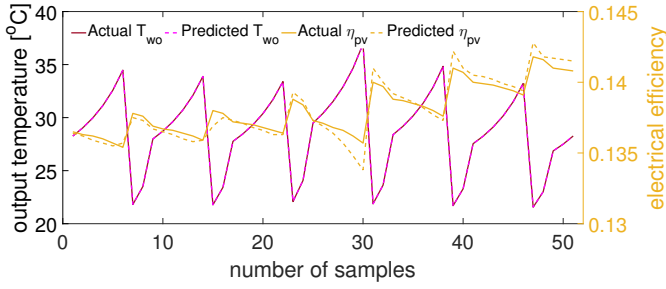


Fig. 8: Comparison of actual and predicted outputs using neural network.

Fig. 9 are chosen. The reference value of the water output temperature is set in order to obtain the control input which is the mass flow of the fluid and PV efficiency (see Fig. 10).

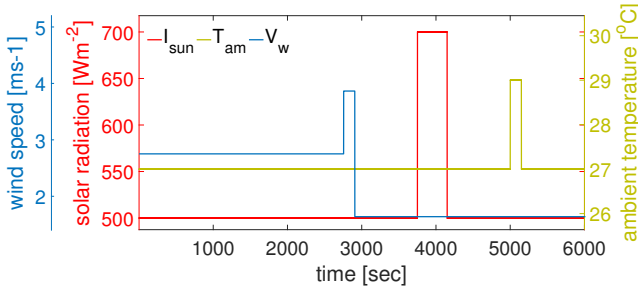


Fig. 9: External inputs imposed on the water-based system.

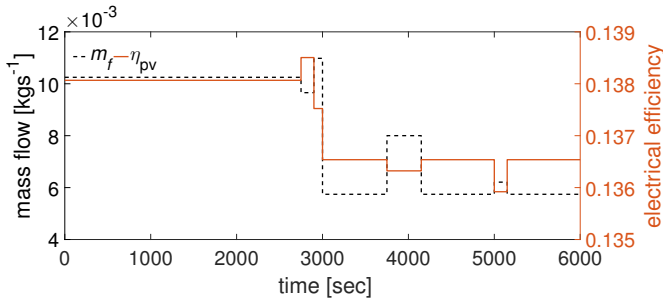


Fig. 10: Evolution of the PV efficiency and control input.

The control input is then injected into the real water-based PV-T mathematical model, and the results in Fig. 11 show that the reference point is perfectly tracked even with the external inputs. Similarly, the corresponding state's temperature evolution using the control input and external inputs is depicted in Fig. 12. To demonstrate the performance of the proposed ANN-based controller, a set of simulations are carried out. The best performance is successfully reached and is checked through mean squared error.

In order to control the system, the first step is to get a NARMA model and predictive model of the system to be controlled. After accepting the generalization of the modeling of the presented structure, testing of the models can be

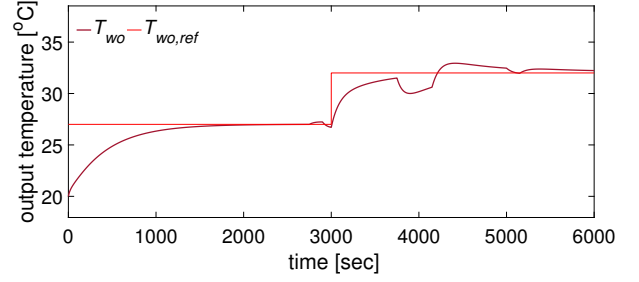


Fig. 11: Evolution of the outlet water temperature and disturbance rejection.

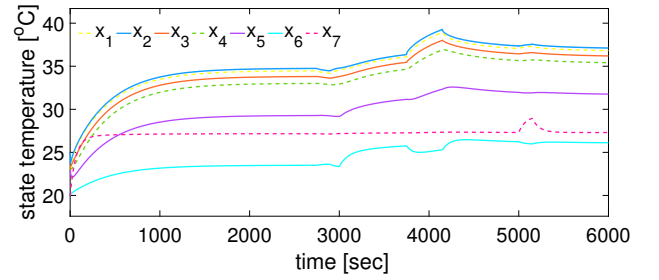


Fig. 12: Evolution of state temperatures.

done with the unseen data. Table II presents the parameters for the predictive controller and NARMA-L2 controller.

TABLE II: Parameters for predictive and NARMA-L2 controllers.

controller	predictive	NARMA-L2
delayed inputs	2	2
delayed outputs	2	2
hidden layer	16	16
ζ	0.05	-
n_2 & n_u	7 & 2	-

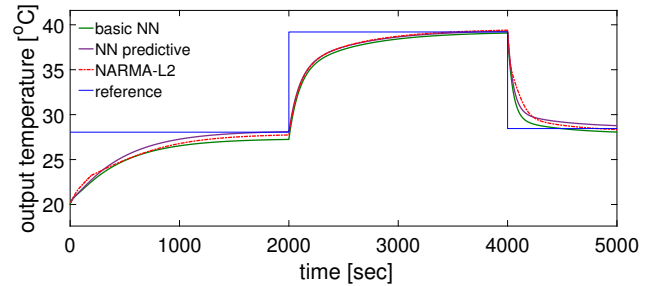


Fig. 13: Response using basic controller, predictive controller and NARMA-L2 controller.

The response of the proposed controllers are compared in Fig. 13. The obtained results indicate that the desired points are tracked by the controllers. It can be observed that the predictive controller is more accurate compared to the other two controllers. However, the performance of the controllers depends on the accuracy of the plant identification. It should

be noted that the designed controllers using neural network are directly implemented into the real mathematical model presented above. The intention is to illustrate a variety of control methods that can be utilized to control the output temperature of the plant.

V. CONCLUSIONS

In this paper, PV-T is modeled using a decision tree algorithm and ANN to describe the system's dynamics represented by physical equations. A key advantage of using AI modeling is that the models can learn patterns and relationships in data. This implies that AI models can often find solutions that may not be readily apparent by traditional mathematical modeling. This approach can handle complex and inconsistent data. Through this paper, it can be concluded that ANN has better accuracy in predicting the outputs compared to the decision tree algorithm.

Designing a controller is a challenging task and AI can be used to accurately track the desired output. A simple neural network control for the collector with uncertain dynamics is presented. The performance of the control techniques has been shown considering different disturbance scenarios. In fact, the disturbances are rejected and the controller tracks the desired output accurately and efficiently.

As a perspective of this work, the presented results will be confronted with physical experimentation to guarantee its feasibility and efficiency in real conditions.

NOMENCLATURE

Symbols

A_{mod}	area
C_w	specific heat capacity
I	input
I_{sun}	solar radiation
T	temperature
T_h	threshold
W	weight
wd	width of collector
y	output of linear combiner

Greek letters

β_p	temperature coefficient
δ	solar radiation coefficient
η_r	reference efficiency

Subscripts

am	ambient
c	PV cell
g	glass cover
i	thermal insulator
m	tube
r	absorber
t	tedlar
w	fluid (water)

ACKNOWLEDGMENT

This work was carried out as part of the SOLARISE project of the Interreg 2 Seas 2014-2020 programme co-

financed by the European Regional Development Fund sub-grant contract No. 2S04-004.

REFERENCES

- [1] J. Alsarraf, H. Moayedi, A. S. A. Rashid, M. A. Muazu, and A. Shah-savar, "Application of pso-ann modelling for predicting the exergetic performance of a building integrated photovoltaic/thermal system," *Engineering with Computers*, vol. 36, no. 2, pp. 633–646, 2020.
- [2] S. Dubey and G. Tiwari, "Thermal modeling of a combined system of photovoltaic thermal (pv/t) solar water heater," *Solar energy*, vol. 82, no. 7, pp. 602–612, 2008.
- [3] A. Tiwari and M. Sodha, "Performance evaluation of solar pv/t system: an experimental validation," *Solar energy*, vol. 80, no. 7, pp. 751–759, 2006.
- [4] M. E. A. Slimani, M. Amirat, I. Kurucz, S. Bahria, A. Hamidat, and W. B. Chaouch, "A detailed thermal-electrical model of three photovoltaic/thermal (pv/t) hybrid air collectors and photovoltaic (pv) module: Comparative study under algiers climatic conditions," *Energy conversion and management*, vol. 133, pp. 458–476, 2017.
- [5] Z. U. Abdin and A. Rachid, "Bond graph modeling of a water-based photovoltaic thermal (pv/t) collector," *Solar Energy*, vol. 220, pp. 571–577, 2021.
- [6] A. Gagliano, G. M. Tina, S. Aneli, and S. Nizetić, "Comparative assessments of the performances of pv/t and conventional solar plants," *Journal of Cleaner Production*, vol. 219, pp. 304–315, 2019.
- [7] T. Brahim and A. Jemni, "Economical assessment and applications of photovoltaic/thermal hybrid solar technology: A review," *solar Energy*, vol. 153, pp. 540–561, 2017.
- [8] Z. U. Abdin and A. Rachid, "A survey on applications of hybrid pv/t panels," *Energies*, vol. 14, no. 4, p. 1205, 2021.
- [9] G. Tiwari and A. Gaur, "Photovoltaic thermal (pvt) systems and its applications," in *2nd international conference on green energy and technology*. IEEE, 2014, pp. 132–138.
- [10] M. Zamen, A. Baghban, S. M. Pourkiaei, and M. H. Ahmadi, "Optimization methods using artificial intelligence algorithms to estimate thermal efficiency of pv/t system," *Energy Science & Engineering*, vol. 7, no. 3, pp. 821–834, 2019.
- [11] M. Abd Elaziz, S. Senthilraja, M. E. Zayed, A. H. Elsheikh, R. R. Mostafa, and S. Lu, "A new random vector functional link integrated with mayfly optimization algorithm for performance prediction of solar photovoltaic thermal collector combined with electrolytic hydrogen production system," *Applied Thermal Engineering*, vol. 193, p. 117055, 2021.
- [12] H. Ravaee, S. Farahat, and F. Sarhaddi, "Artificial neural network based model of photovoltaic thermal (pv/t) collector," *The journal of mathematics and computer science*, vol. 4, no. 3, pp. 411–417, 2012.
- [13] A. Shahsavar, H. Moayedi, A. H. Al-Waeli, K. Sopian, and P. Chelvanathan, "Machine learning predictive models for optimal design of building-integrated photovoltaic-thermal collectors," *International Journal of Energy Research*, vol. 44, no. 7, pp. 5675–5695, 2020.
- [14] D. Kamthania and G. Tiwari, "Determination of efficiency of hybrid photovoltaic thermal air collectors using artificial neural network approach for different pv technology," *BIJIT*, vol. 4, no. 1, pp. 397–404, 2012.
- [15] A. C. Megri and I. El Naqa, "Prediction of the thermal comfort indices using improved support vector machine classifiers and nonlinear kernel functions," *Indoor and Built Environment*, vol. 25, no. 1, pp. 6–16, 2016.
- [16] S. Xu, S. Hashimoto, Y. Jiang, K. Izaki, T. Kihara, R. Ikeda, and W. Jiang, "A reference-model-based artificial neural network approach for a temperature control system," *Processes*, vol. 8, no. 1, p. 50, 2020.
- [17] M. Rakhra, P. Soniya, D. Tanwar, P. Singh, D. Bordoloi, P. Agarwal, S. Takkur, K. Jairath, and N. Verma, "Crop price prediction using random forest and decision tree regression:-a review," *Materials Today: Proceedings*, 2021.
- [18] M. Abdurohman, A. G. Putrada, and M. M. Deris, "A robust internet of things-based aquarium control system using decision tree regression algorithm," *IEEE Access*, 2022.
- [19] M. Elsis, "Design of neural network predictive controller based on imperialist competitive algorithm for automatic voltage regulator," *Neural Computing and Applications*, vol. 31, no. 9, pp. 5017–5027, 2019.
- [20] M. George and K. P. Basu, "Narma-12 controlled variable frequency three-phase induction motor drive," *European Journal of Scientific Research*, vol. 70, no. 1, pp. 98–111, 2012.